Polarimetry of γ-Rays Converting to e^+e^- Pairs with Silicon-Pixel-Based Telescopes

Denis Bernard,

Laboratoire Leprince-Ringuet (LLR)

Nucl.Instrum.Meth.A 1066 (2024) 169590

11th International Fermi Symposium, College Park, Sept. 9-13, 2024

MeV γ-Ray Polarimetry: Science Goals

- Main targets: bright sources, deciphering emission mechanism
  - Blazars:
    leptonic synchrotron self-Compton (SSC) or **hadronic** (proton-synchrotron)
    Zhang and Böttcher, Astrophys.J. 774, 18 (2013)
  - Pulsars: Tagging the onset of Curvature Radiation (CR)
    Harding and Kalapotharakos, Astrophys. J. 840 73 (2017)
- Further away (pending on statistics)
  - LIV search (Lorentz-invariance violation), induced dilution of the GRB polarization signal during propagation F. Kislat, arXiv:1907.06514 [astro-ph.HE],
  - Axion search, A. Rubbia and A. S. Sakharov, Astropart. Phys. **29** (2008) 20
    ALPs (Axion-like particles) G. Galanti, Universe **10** (2024) 312

Polarimetry

$$\frac{\mathrm{d}\Gamma}{\mathrm{d}\phi} \propto (1 + AP\cos\left[2(\phi - \phi_0)\right]),$$

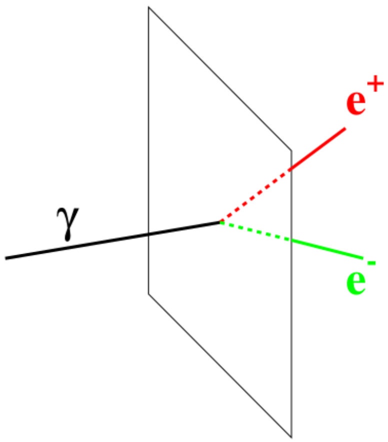

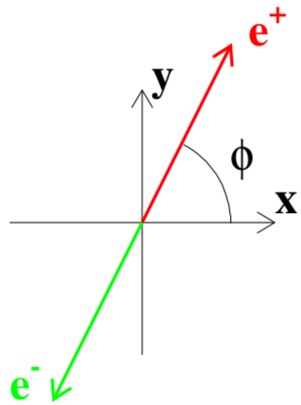

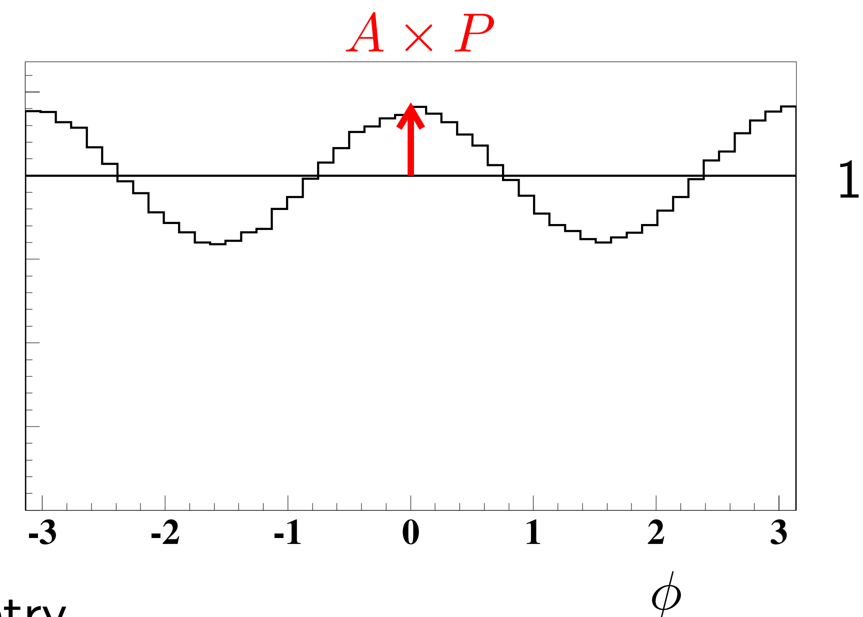

- P source linear polarisation fraction
- A γ-ray conversion polarization asymmetry
- ϕ event azimuthal angle
- ϕ_0 source polarization angle.

QED Polarization asymmetry

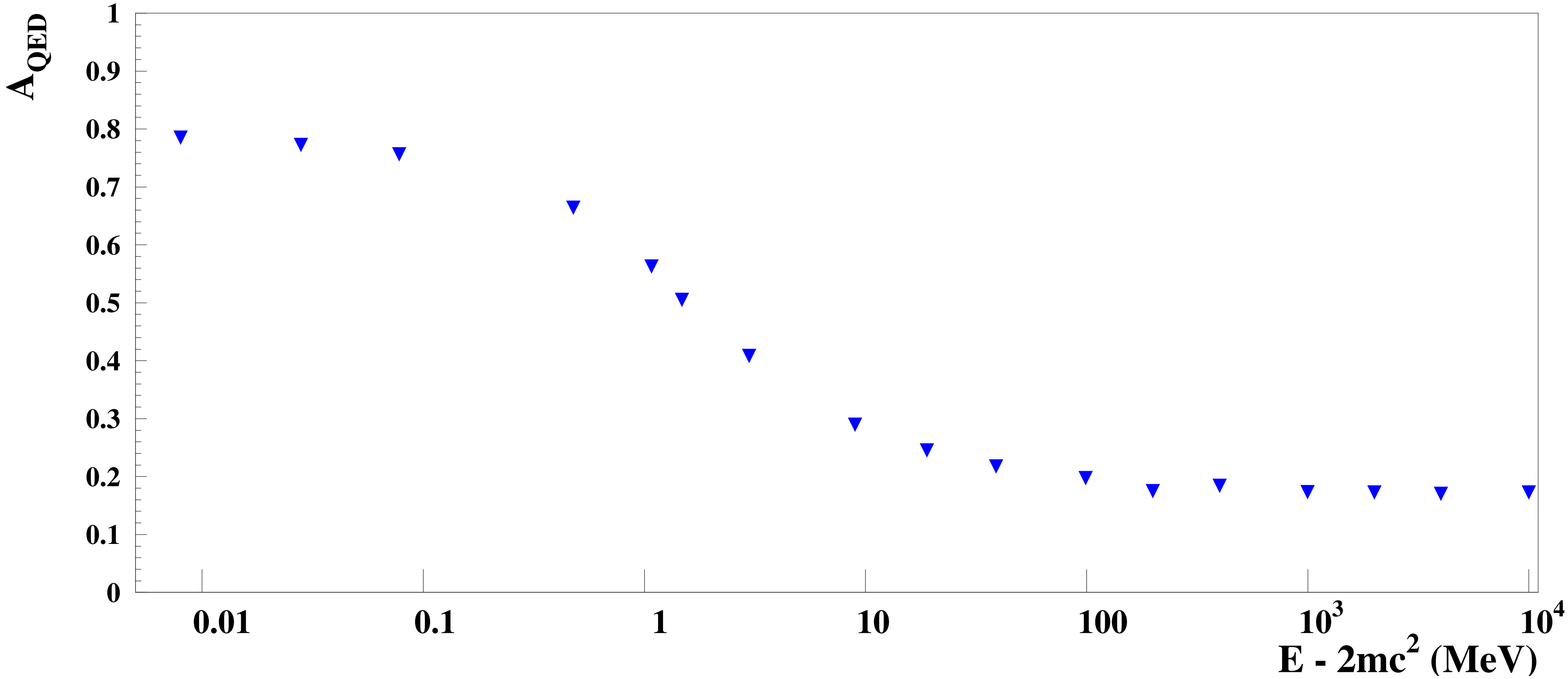

Close to 0.2 in energy range within reach

Polarimetry with pairs: e^+ and e^- Multiple Scattering

Simulated γ-ray conversion
In homogeneous medium

$\gamma \rightarrow$ 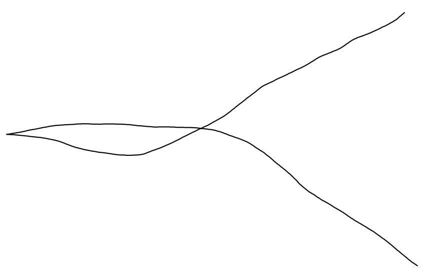

$$D = A/A_{\mathrm{QED}}$$

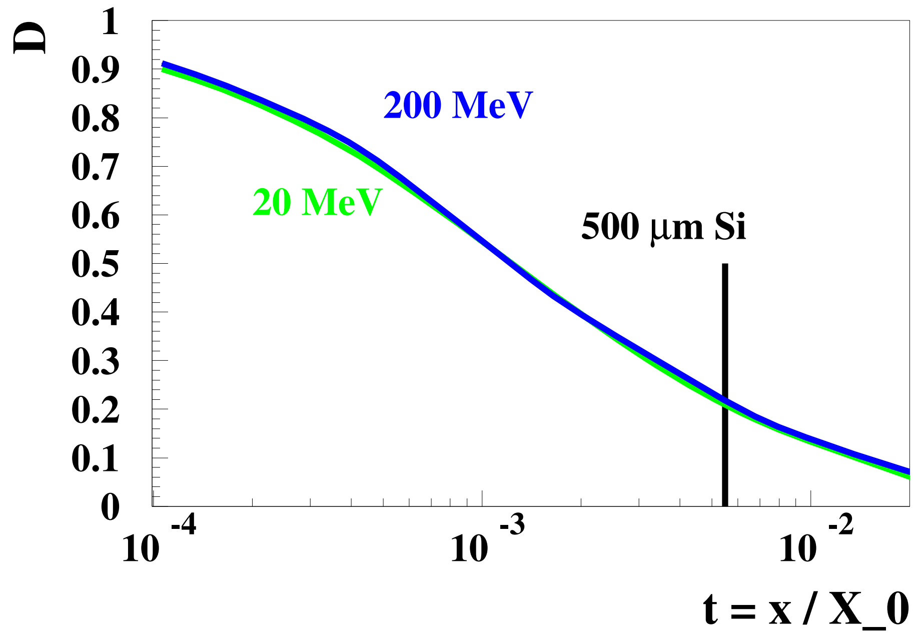

Adapted from D.Bernard, Nucl. Instrum. Meth. A 729 (2013) 765

Dilution, D, as a function of pathlength after conversion, normalized to radiation length, t

Most polarimetry information lost before leptons exited conversion wafer

Performance of Silicon Strip detectors: The Fermi-LAT

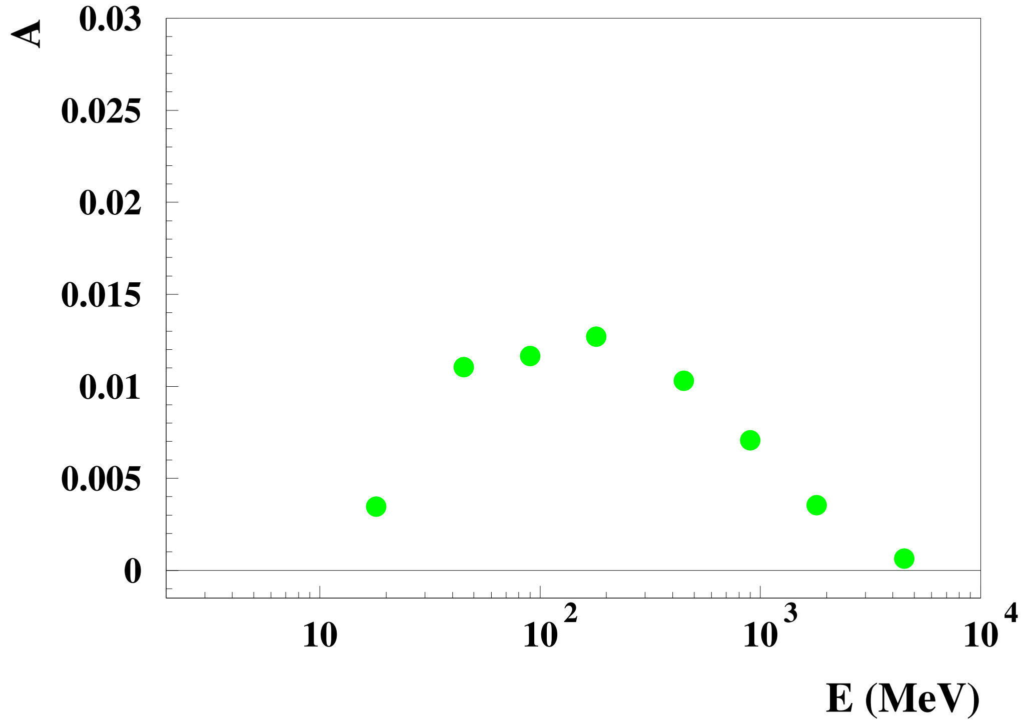

- Effective asymmetry peaks at $A \approx 0.0125$ for $\approx 200\,\text{MeV}$
- A dilution factor A/A_{QED} of a factor of 0.07
- Expected $\sigma_{\text{P}} \approx \mathbf{0.15}$ on bright source, $1.5 \times 10^{-3}\text{MeV}\text{cm}^{-2}\text{s}^{-1}/E^2$, exposure $\epsilon \approx 2 \times 10^{11}\text{cm}^2\text{s}$

D. Bernard, Fermi Symposium 2022 and Nucl. Instrum. Meth. A **1042** (2022) 167462 (Fig. 21)

Estimate confirmed with full *Fermi*-LAT study (Vela, 15 years), A. Laviron+ PoS ICRC2023 (2023) 721 and Talk at this Symposium

Strips $\rightarrow$ *Pixels*

		Fermi-LAT	AMEGO-X
	Layer	2 single-sided SSD	Pixels
	Converter ?	Tungsten foils	All Si (no Tungsten foils)
e	Si Thickness (μm) per layer	$2 \times 400 = 800$	500
p	Pitch / size (μm)	228	500
d	Layer spacing (cm)	3.3	1.0

Analysis

– Pair conversions selected (Compton rejected) based on MC information

– No additional trigger emulation

– **Track reconstruction based on information in conversion layer + next layer**

As in my previous D. Bernard, Nucl. Instrum. Meth. A **1042** (2022) 167462

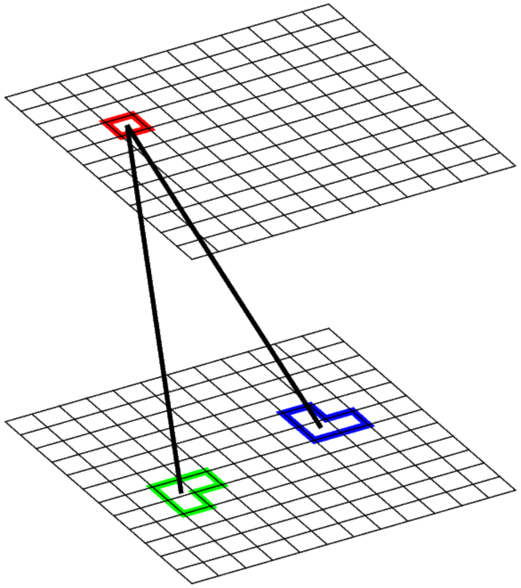

– Pixels with > 0 deposited energy recorded.

– Recorded pixels with a side in common clustered

– **Exact number of clusters required**

- 1 in conversion layer
- 2 in next layer

– Track directions reconstructed from (geometric) cluster barycenters

– Event azimuthal angle computed from track azimuthal angles

Event Fractions

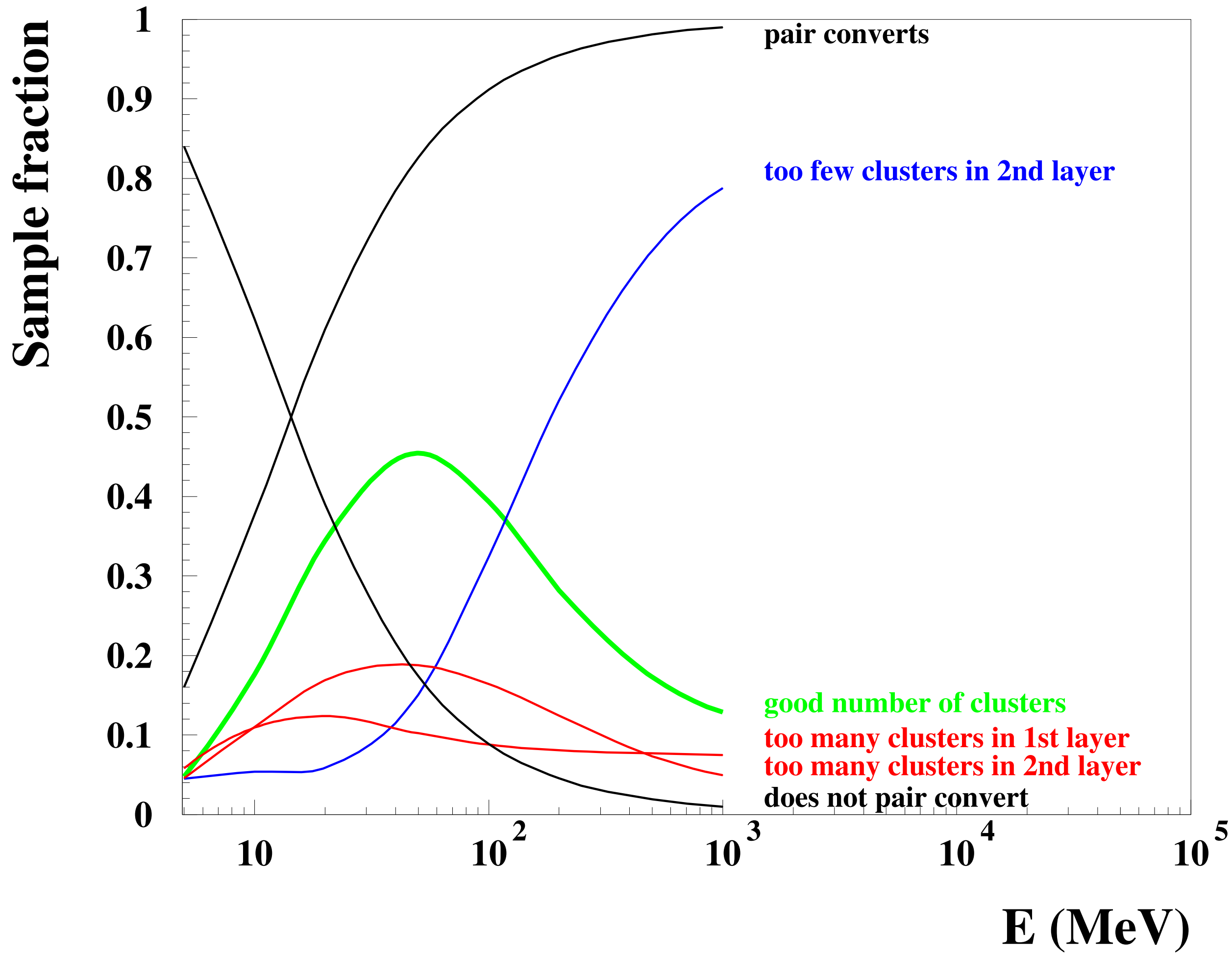

- Selection efficiency peaks at $\approx 45\,\%$ for $E \approx 50\,$MeV
- Drops at low energies due to Compton scattering prior to conversion
- Drops at high energies due to both tracks create same cluster in next layer

Results

Selection efficiency
ϵ

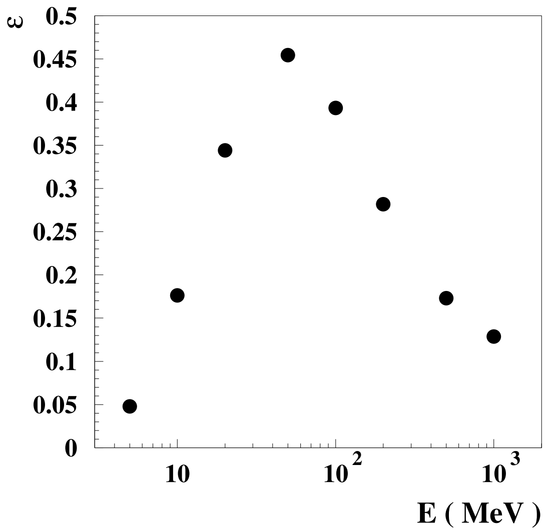

Polarization asymmetry
A

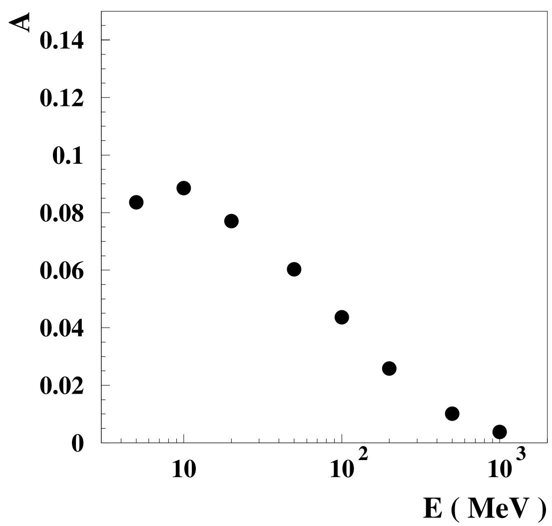

Figure of Merit
$\epsilon \times A^2$

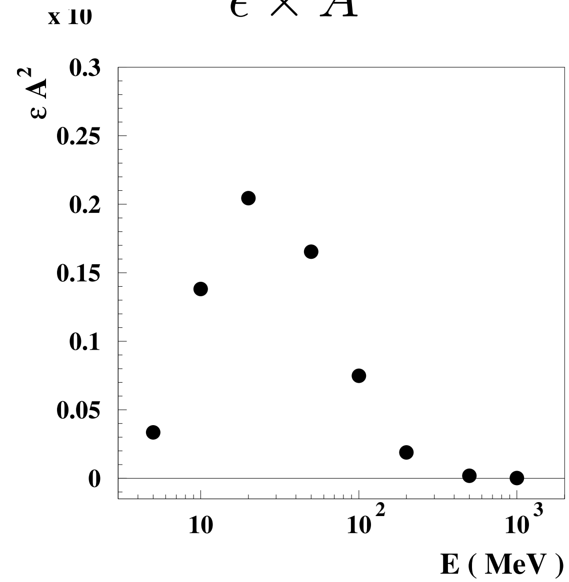

- A plateaus at ≈ 0.09 at low energies, dilution factor $D = A/A_{\mathrm{QED}} \approx 1/3$
- Figure of merit peaks for $E \approx 20\,$MeV (sizable between 10 – 100 MeV)

Energy-Integrated Performance

Energy bins, E_k, events weighted with weight A_k, $\Rightarrow$

$$\sigma_P = \sqrt{\frac{2}{\sum_k A_k^2 N_k}} \qquad N_k = \frac{\eta\, \epsilon_k\, F_0\, \Delta E_k\, H(E_k)\, T\, m}{E_k^2},$$

- Differential flux F_0/E^2, $F_0 = 10^{-3}\,\mathrm{MeV}/(\mathrm{cm}^2\mathrm{s})$,
- m detector silicon mass (g), T duration (s)
- $H(E_k)$ total photon attenuation $(\mathrm{cm}^2/\mathrm{g})$ at photon energy E_k NIST XCOM data base

  (i.e. effective area per unit mass)
- ΔE_k width of energy bin k, ϵ_k selection efficiency,
- Exposure factor $\eta = (1 - \cos(\theta_{\mathrm{cut}}))/2 \approx 0.375$.

Energy-integrated figure of merit, $\sum_k A_k^2 N_k/(T\, m) = 81.(\text{year} \cdot \mathrm{kg})^{-1}$,

For a 5 year, 30 kg AMEGO-X mission, $\sigma_P \approx 0.013$ within reach.

Energy-Integrated Performance: Variation with Detector Parameters

Energy-integrated figure of merit, $\sum_k A_k^2 N_k/(T\,m)$

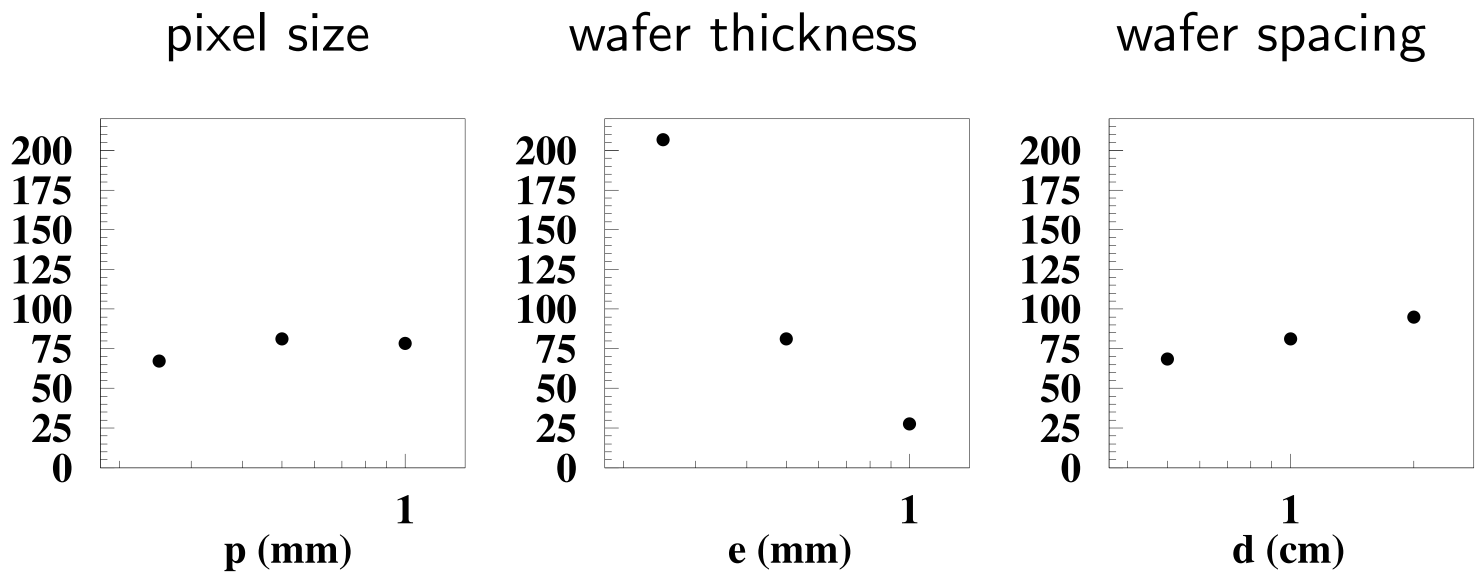

- Driving parameter of the overall performance is clearly wafer thickness e.

  (Total silicon mass kept constant)

Conclusion

– Performance of Silicon-pixel based pair polarimeter estimated with simple model

– Main performance driving parameter, wafer thickness

– Excellent prospects for the brightest sources of the MeV gamma-ray sky.

$$\sigma_P = \begin{array}{lll} 0.15 & (\text{ LAT} & 15\,\text{years }) \\ 0.013 & (\text{ AMEGO-X} & 5\text{ years }) \end{array}$$

On a bright Crab-like source.

Back-up slides

Deciphering Emission Mechanism in Blazars with γ-Ray Polarimetry

- Blazars: active galactic nuclei (AGN) with one jet pointing (almost) to us

leptonic synchrotron self-Compton (SSC)

or

hadronic (proton-synchrotron) ?

- high-frequency-peaked BL Lac
- X band: 2 -10 keV
- γ band: 30 - 200 MeV
- SED's indistinguishable, but
  - X-ray: $P_{\text{lept}} \approx P_{\text{hadr}}$
  - γ-ray: $P_{\text{lept}} \ll P_{\text{hadr}}$

Zhang and Böttcher, Astrophys.J. 774, 18 (2013)

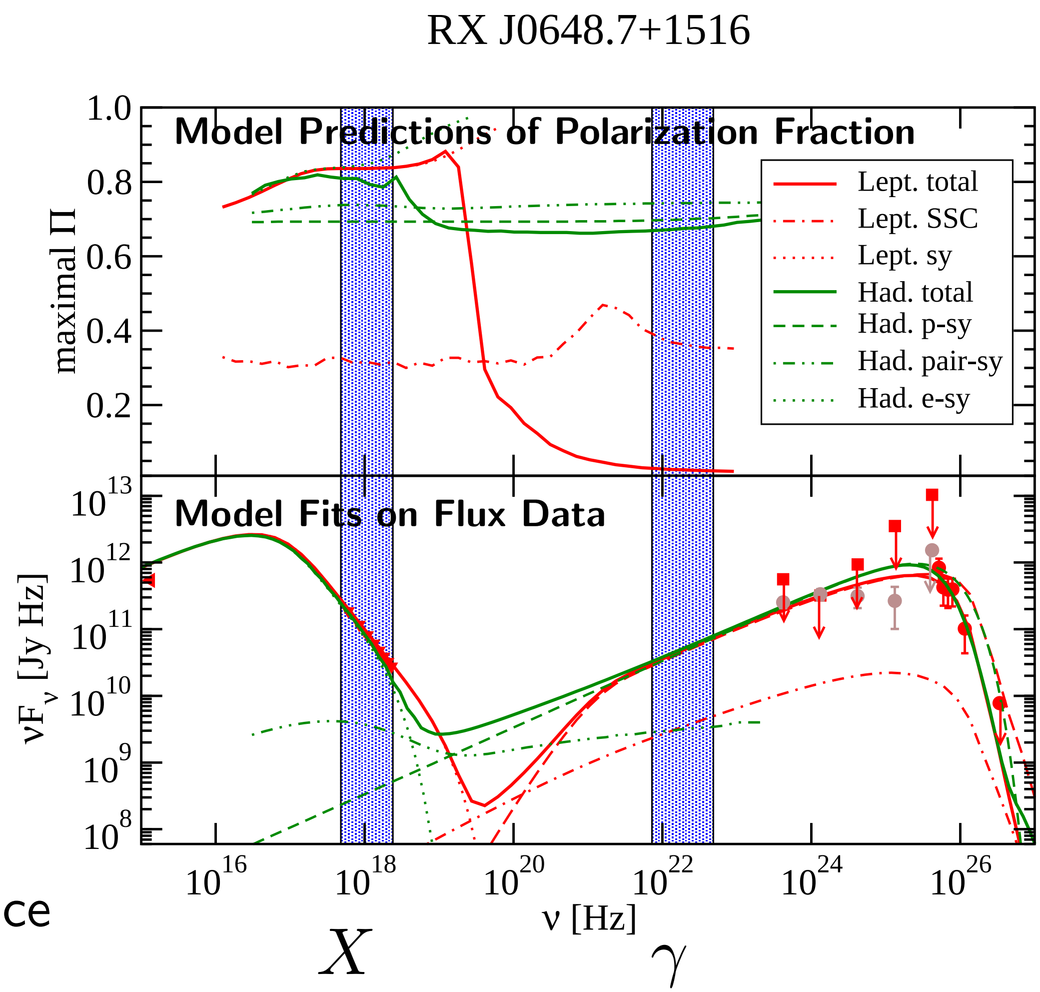

"Maximal" Π: assumes no $\vec{B}$ turbulence

Tagging the (Curvature Radiation CR – Synchrotron Radiation SR) Transition in Rotation-Powered Pulsars

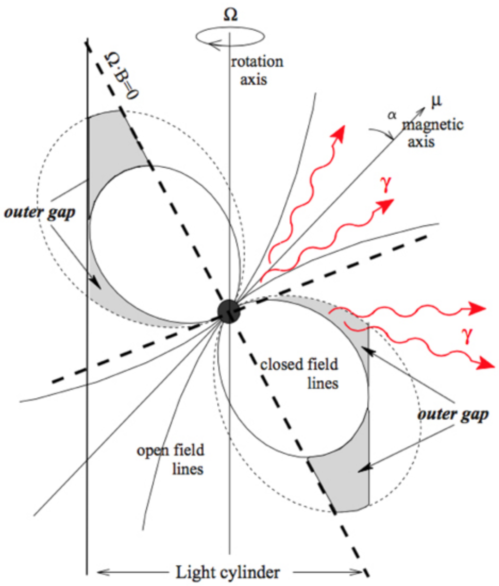

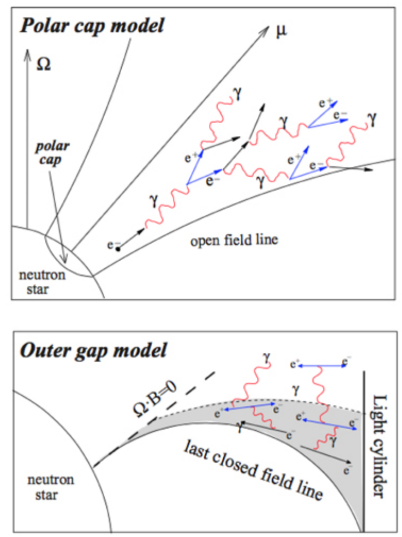

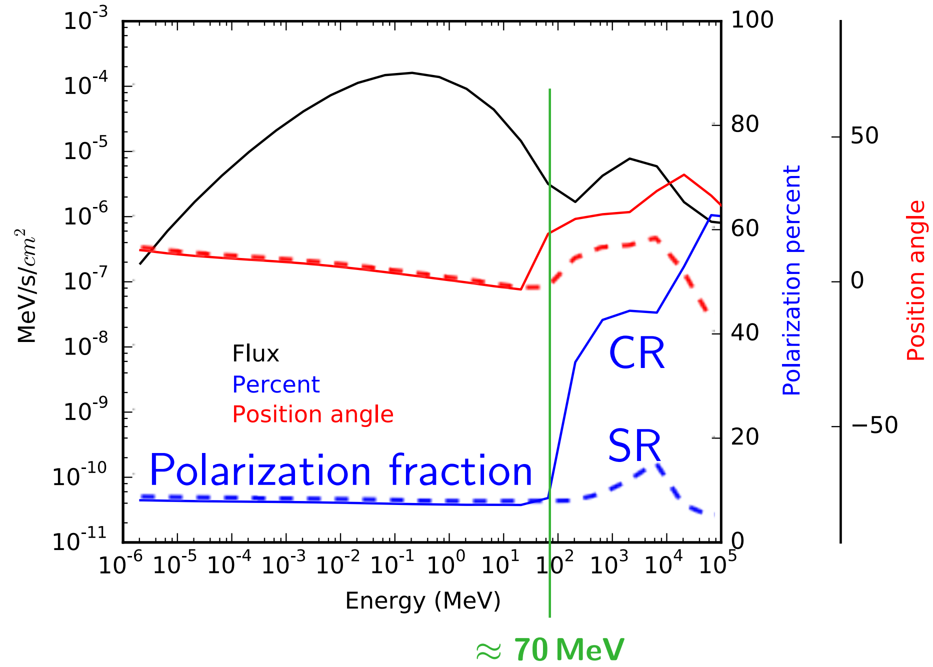

Polar-cap model of Crab-like pulsar

- MeV component is SR from pairs
- GeV component is either CR (solid line) or SR (dashed line)

Harding and Kalapotharakos, Astrophys. J. 840 73 (2017)

Pair Opening Angle: 1/E Scaling

(pair opening angle) × (photon energy)

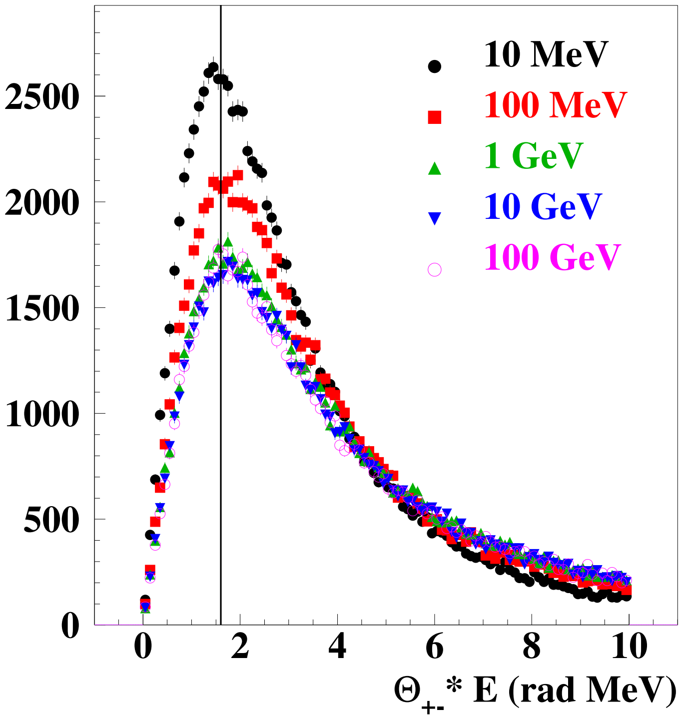

Vertical line: high-energy asymptotic most probable value

$$\frac{1.6 \text{ rad} \cdot \text{MeV}}{E}$$

H. Olsen, Phys. Rev. 131 (1963) 406

D. Bernard, Nucl. Instrum. Meth. A **899** (2018) 85

Tracking: Single-Track Polar-Angle Resolution

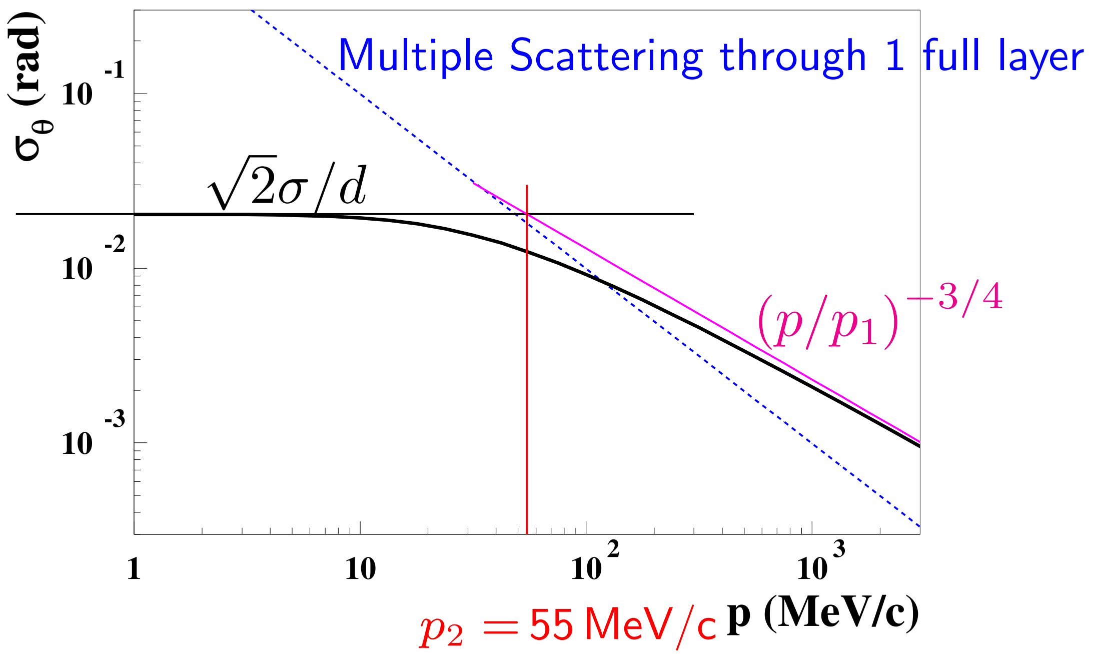

Curve, angular resolution of optimal (Kalman filter) tracking, eq. (1) of arXiv:1902.07910

- for conversion at the very bottom of a layer,
- an asymptotically large number of planes, and
- dE/dx energy loss neglected

A two-layer measurement is close to optimal at low track p (low photon E)

Optimal Sample Combination

$\frac{d\Gamma}{d\phi} \propto (1 + AP\cos 2\phi)$, $\Rightarrow$ $P = \sum_i^N w_i/(A \times N)$ with weight $w_i \equiv 2\cos 2\phi_i$

K samples. Weight each with inverse variance , $P = \left(\sum_k \frac{P_k}{V_k}\right) / \left(\sum_k \frac{1}{V_k}\right)$, with $\frac{1}{V_k} = \frac{N_k A_k^2}{2}$

(eg. D. J. Shahar Open J. Stat. 2017, 7, 216.)

So, $P = \sum_k \sum_i^{N_k} w'_{i,k}$ with $w'_{i,k} = \frac{A_k w_{i,k}}{\sum_\ell N_\ell A_\ell^2}$, precision $\sigma_P = \sqrt{\frac{2}{\sum_k N_k A_k^2}}$

Weight each event by the average asymmetry of the sample to which it belongs.

Figure of merit of sample k, $N_k A_k^2$, of total sample, $\sum_k N_k A_k^2 = N \sum_k \epsilon_k A_k^2$.

Method

ASAP: As Simple As Possible

- Target
  - "Infinite" number of "infinite" Si planes, $z < 0$

    $\Rightarrow$ All photons convert, (thin detector, effective area $\propto$ silicon mass)
  - Dead material neglected
- Point-like source,
- Isotropic exposure map with $\cos\theta > 0.25$ cut (approx $\theta < 75^\circ$)
- Assume the telescope provides γ sample associated with known
  - γ direction (exactly, that of the source) and
  - γ energy
- Electromagnetic physics simulation EGS5, version 1.0.5, H. Hirayama *et al.*, SLAC-R-730, 2005
- No background

Wafer Thickness e Variation

Number of incident photons, therefore effective area, therefore Si mass, kept unchanged

Selection efficiency ϵ | Polarization asymmetry A | Figure of Merit $\epsilon \times A^2$

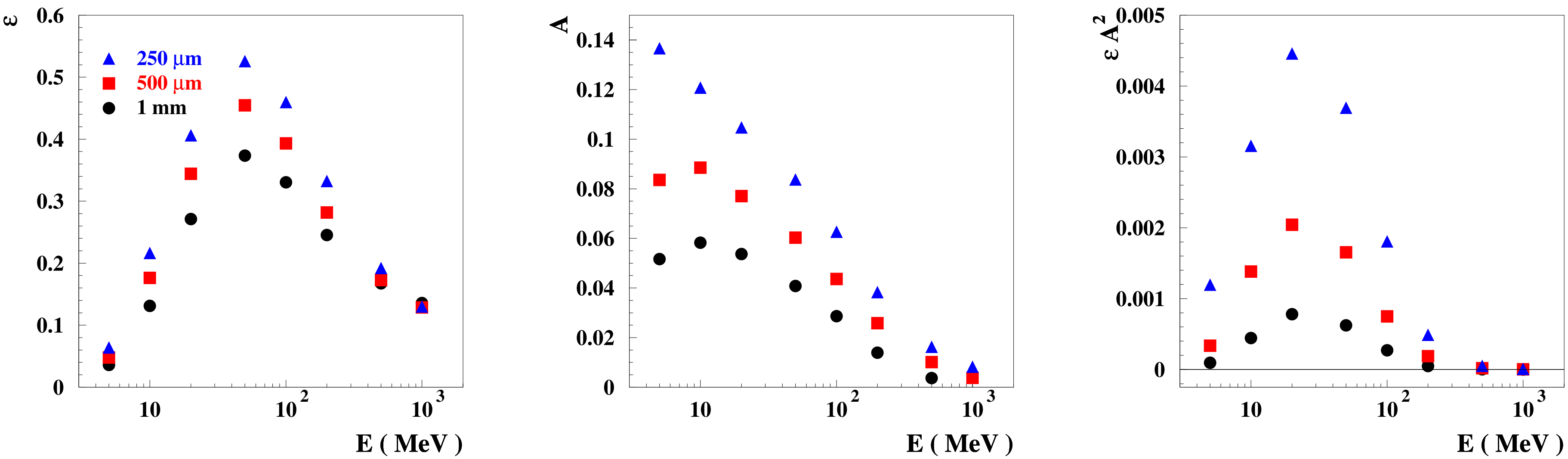

- ϵ decreases mildly with increasing e (increase of the fraction of events with too large a number of clusters in the 2nd layer)
- A decreases with increasing e due to multiple scattering

Layer Spacing d Variation

Selection efficiency ϵ	Polarization asymmetry A	Figure of Merit $\epsilon \times A^2$

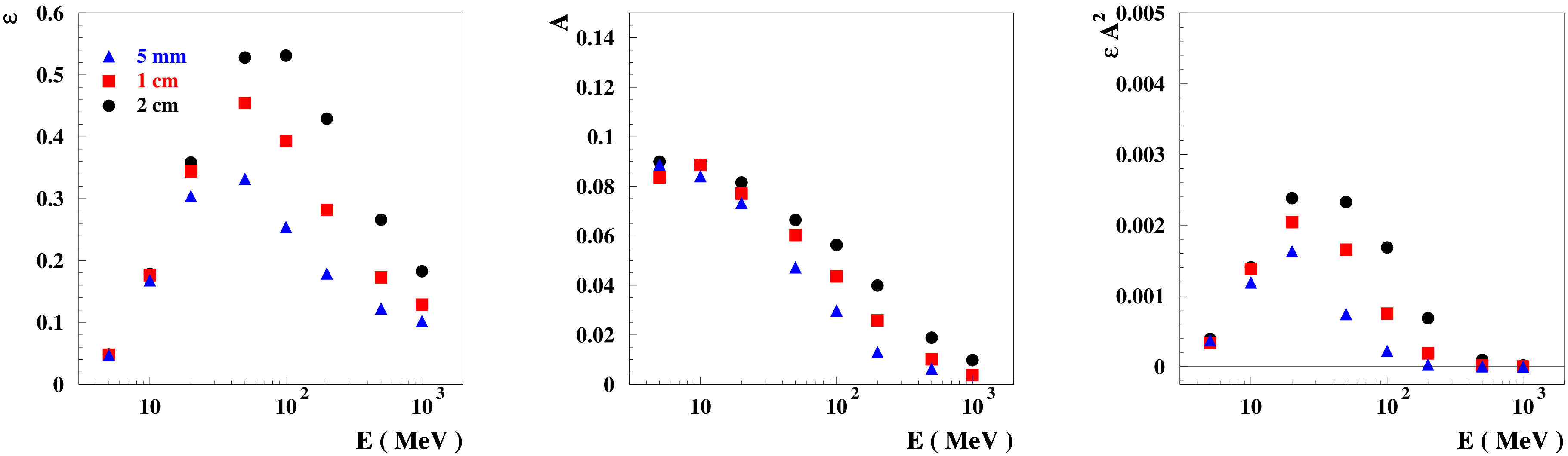

- Increasing the wafer spacing obviously improves the selection efficiency at high energies (better separation of small opening angles)
- A barely affected, except at high energy

Pixel Size p Variation

Selection efficiency ϵ | Polarization asymmetry A | Figure of Merit $\epsilon \times A^2$

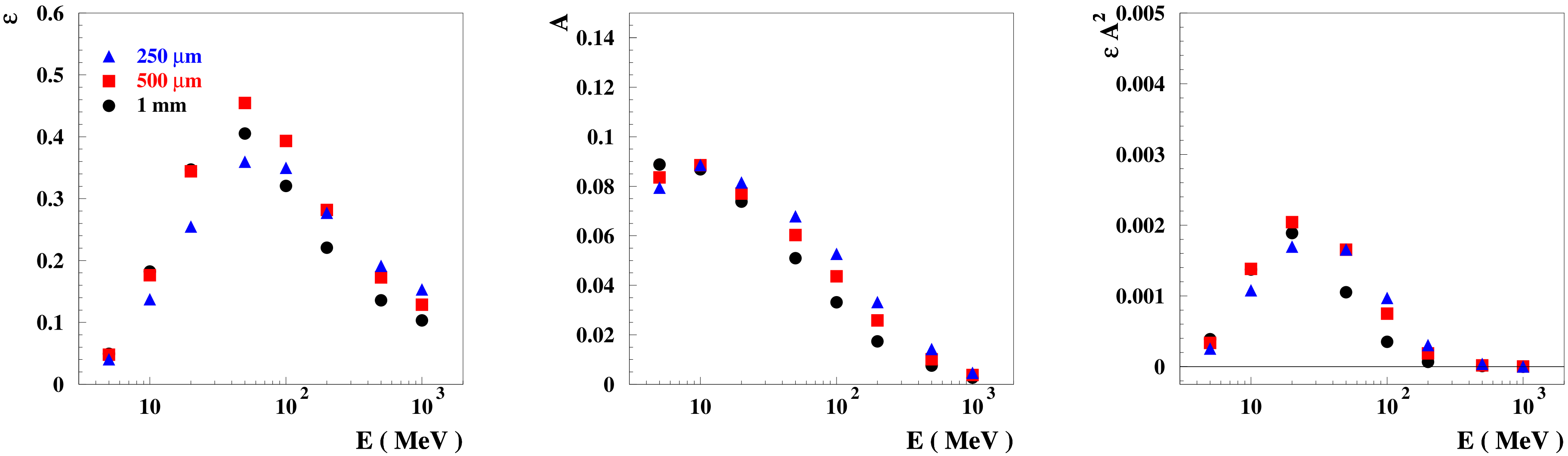

- Smaller pixels improves mildly ϵ at high energy (better separation of small opening angles)
- Smaller pixels degrades mildly ϵ at low energy (larger fraction of events with too many clusters in the 2nd wafer).
- A barely affected (the additional contribution of the pixel size to the ϕ angular resolution not the dominant factor) except at high energy